Performance Evaluation of the 5G LDPC and RS Codes in a Pre-Amplified PPM Receiver

Konstantinos Yiannopoulos
Department of Informatics and Telecommunications
University of the Peloponnese
Tripoli, Greece
kyianno@uop.gr

Antonios Aspreas
Department of Informatics and Telecommunications
University of the Peloponnese
Tripoli, Greece
aspreasant@uop.gr

Nikos C. Sagias
Department of Informatics and Telecommunications
University of the Peloponnese
Tripoli, Greece
nsagias@uop.gr

2022 Panhellenic Conference on Electronics & Telecommunications (PACET) | 979-8-3503-9958-5/22/$31.00 ©2022 IEEE | DOI: 10.1109/PACET56979.2022.9976320

***Abstract*—We present results for the performance of a pre-amplified optical receiver using LDPC and RS error correction codes. The LDPC codes under consideration were recently proposed for the 5G communication standard and their construction is suitable for correcting the burst errors that are introduced by PPM. The results show that the LDPCs can provide a very significant coding gain in comparison with the uncoded system. They also perform better than RS codes of an equal code rate and equivalent data block size.**

***Index Terms*—Optical Amplifier, Pulse Position Modulation, Low Density Parity Check Codes, Reed Solomon Codes**

I. Introduction

Optical technologies are being envisaged as an alternative to radio for the implementation of reliable, high-capacity space communication links and recent demonstrations have employed highly sensitive optical receivers to successfully transfer data at unpreceded rates [1], [2], [3], [4]. Some of the key communication technologies that were utilized include optical amplification, orthogonal modulation such as pulse position modulation (PPM) and coding, which all aim to reduce the power that is required to achieve low bit error probabilities (BEPs) at the receiver.

The advances in coding have demonstrated the capability of constructing codes that perform close to the Shannon limit. Low Density Parity Check (LDPC) codes, in particular, demonstrate such potential [5] and recently they were included for channel coding in the 5G standard [6]. The LDPC code construction that is presented within the standard results in a parity-check matrix that constitutes of smaller block sub-matrices. The sub-matrices are cyclic permutations of the identity matrix of size $Z_c \times Z_c$, where Z_c is the lifting size, and this construction method ensures that the parity checks are never performed on successive bits. This is important for PPM, since a single symbol error may cause an error burst of up to consecutive $\log_2 Q$ bits, where Q is the modulation order. Assuming that $Z_c \gg \log_2 Q$, which is expected for practically considered PPM orders and data blocks, the bits of the error burst will participate in different parity checks and can be corrected independently.

In the current work, we assess via Monte Carlo (MC) simulations the performance of the 5G LDPC codes in an optically pre-amplified PPM receiver. LDPC codes have been previously studied with PPM for receiver models that include the Poisson and Gaussian [7], [8], [9], [10], [11], [12], however we consider a more accurate model for the pre-amplified PPM receiver that relies on χ^2 statistics [13], [14]. χ^2 statistics complicate the calculation of the likelihoods that are required at the LDPC decoder [15], since the corresponding likelihood function involves the evaluation of a generalized hypergeometric series. We maintain the exact relations for the likelihood functions and accurately simulate the significant coding gain that can be achieved from the utilization of LDPC codes under χ^2 signal reception. Moreover, we compare the 5G LDPC codes with Reed Solomon (RS) ones, which also have the capability of correcting the burst errors introduced by PPM [7]. Our results show that the LDPCs perform better than the RS codes in all simulated scenarios that involve 4- and 16-PPM, coding rates of $1/3$ and $2/3$, and varying bandwidth optical filters. The relative improvement of LDPCs is dependent on the three aforementioned parameters, and their use favored by higher modulation orders, lower coding rates and narrower optical filters.

The rest of this paper is structured as follows: Section II discusses the LDPC code construction of the 5G standard, as well as RS codes. The χ^2 reception model is also described in detail, along with the required modifications in the likelihood function and log-likelihood-ratios (LLRs) that are required to utilize the binary LDPC decoder in PPM modulation and χ^2 statistics. The MC simulation results are presented in Section III, along with the performance comparison of LDPC and RS codes. Finally, Section IV summarizes the findings and concludes the paper.

II. System Models

The setup under consideration is shown in Fig. 1. The data are encoded using LDPC or RS codes and the resulting codeword is partitioned in PPM symbols. At the receiving side, the symbols are amplified and optical noise is added by the amplifier. The signal is filtered in the optical domain and the noisy symbols are detected on a photodiode. The electrical current

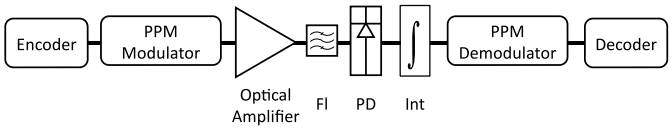

Fig. 1: Setup for the optically pre-amplified PPM communication system. Fl: optical filter, PD: photodiode, Int: integrator.

is integrated over each PPM slot duration, and the resulting signal values are utilized by the demodulator to estimate the transmitted PPM symbol and the corresponding bits. The received bits are grouped into codewords which are processed by the decoder to reconstruct the original data stream. The encoder/decoder, receiver and modulator/demodulator operations are presented in more detail in the following sub-sections.

A. RS and LDPC Codes

In the RS coded system, the data bits are grouped into k symbols of m bits each, and the RS encoder generates codewords of $n = 2^m - 1$ symbols. We select RS codes with $m = 8, 9, 10$ so that $m > \log_2 Q$ and multiple PPM symbols are mapped to a single RS symbol. As a result, it is possible to correct up to $m/\log_2 Q$ consecutive erroneous PPM symbols whenever they are located within the same RS symbol, since this will be perceived as a single error at the decoder. The decoder uses the Berlekamp–Massey algorithm for error correction and is capable of correcting up to $(n-k)/2$ symbol errors per codeword.

For the LDPC system, the quasi-cyclic parity-check matrix structure of the 5G standard is used to generate the codewords [6]. We consider data blocks between 720 and 7040 bits, thus we utilize both Base Graph (BG) structures of the standard and assess the performance for several combinations of lifting sizes Z_c and bits per block K_b. The combinations of parameters are summarized in Table I and are selected so that the resulting block sizes are similar to the ones of the RS codes. The information block columns are always fixed to K_b (10 or 22), depending on the BG selection, so as to avoid padding the data blocks. The desired code rate (CR) is achieved by selecting the first K_b/CR block columns and $K_b(1-CR)/CR$ block rows of the parity-check matrix. The encoder utilizes the double-diagonal structure of the core parity sub-matrix to calculate the core parity bits, while the extension parity bits are calculated via substitution from the extension parity sub-matrix. In contrast with the 5G standard, the codeword is not shortened/punctured and all the bits are transmitted to the decoder. The decoder is based on the min-sum iterative message passing algorithm [16, eq. (1)] and utilizes the log-likelihoods-ratios (LLRs) that are generated at the PPM demodulator using the methodology that is presented in the next section. The maximum number of iterations at the decoder is limited to 10 [8], which provides an acceptable trade-off between performance loss and execution time [17].

TABLE I: LDPC Code Parameter

Data Block (bits)	Code Rate	BG	$\mathbf{i_{LS}}$	$\mathbf{K_b}$	$\mathbf{Z_c}$
720	1/3	2	4	10	72
1600	1/3	2	2	10	160
3520	1/3	2	5	10	352
1280	2/3	2	0	10	128
2880	2/3	2	4	10	288
7040	2/3	1	2	22	320

B. Receiver and Demodulator Models

We consider an IM/DD receiver, where the incoming optical signal is optically amplified and filtered prior to square law detection. The optical signal is modulated using PPM and each PPM symbol comprises Q successive time-slots. One of the slots carries the symbol energy and all other slots are considered empty. At the output of the amplifier, the energy containing slot is magnified by the amplifier gain G and all slots are corrupted by the amplifier noise. The optical signal is converted to electrical in a square law detector and the detector output is integrated over the duration of the slot, to generate the signal vector $\mathbf{s} = (s_1, s_2, \ldots, s_Q)$ for each received symbol.

The s vector components correspond to central $\chi^2_{k,0}$ random variables (RVs) in the $Q-1$ slots that do not have any signal energy, and a non-central $\chi^2_{k,\lambda}$ RV in the slot that has the signal energy. The corresponding pdfs are [14]

$$\begin{aligned} p_e\left(x;k\right) &= \frac{x^{k-1}}{(k-1)!}\, e^{-x}\,, \\ p_s\left(x;k,\lambda\right) &= e^{-(x+\lambda)}\, \left(\frac{x}{\lambda}\right)^{\frac{k-1}{2}}\, I_{k-1}\Big(2\sqrt{\lambda\, x}\Big)\,, \end{aligned} \tag{1}$$

where $I_n(\cdot)$ denotes the modified Bessel function of the first kind. In the previous equations $\lambda = E/N_0 = E_b/N_0\, \log_2 Q$ is the symbol energy to noise ratio, E_b is the energy per bit after amplification, $N_0 = n_{sp}\, h\, f\, (G-1)$ is the optical noise spectral density and k are the noise modes.

In the RS coded system, the demodulator selects the symbol based on the s_i with the highest likelihood and reports the corresponding $\log_2(Q)$ bits to the decoder. In χ^2 statistics the likelihood function is calculated from

$$\begin{aligned} \Lambda\left(s_i;k,\lambda\right) &= \frac{p_s\left(s_i;k,\lambda\right)}{p_e\left(s_i;k\right)} = e^{-\lambda}\,(k-1)!\,\frac{I_{k-1}\big(2\sqrt{\lambda\, s_i}\big)}{\big(\sqrt{\lambda\, s_i}\big)^{k-1}} \\ &= e^{-\lambda}\,{}_0F_1(;k;\lambda\, s_i)\,, \end{aligned} \tag{2}$$

where ${}_pF_q(a_1,\ldots,a_p;b_1,\ldots,b_q;z)$ is the generalized hypergeometric function. The function is increasing with respect to s_i and, as a result, the demodulator makes the selection based on $\max\{s_i\}$.

The min-sum LDPC decoder, on the other hand, requires a log-likelihood-ratio to be associated with each received bit within the PPM symbol. Assuming that the symbols have equal

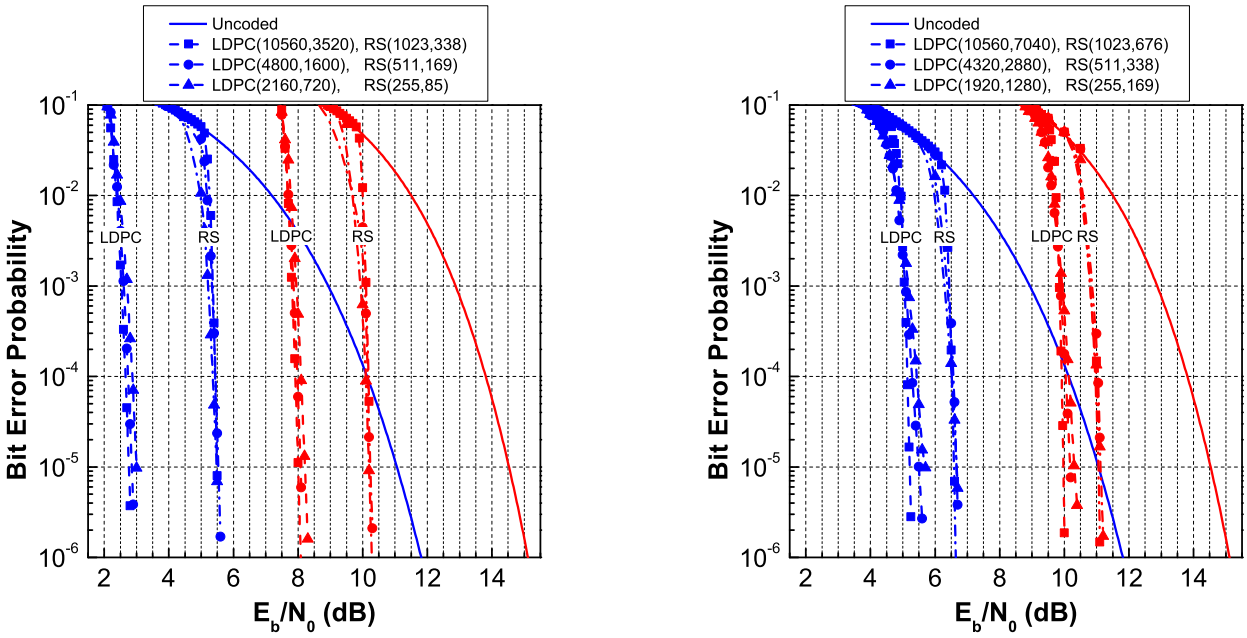

Fig. 2: BEP for the RS and LDPC coded pre-amplified 4-PPM receiver. The blue and red colors correspond to $k = 2$ and $k = 40$ noise modes, respectively.

probabilities, then the a-priori probability for a given symbol equals [18, eq. (10)]

$$P(s_i|\mathbf{s}) = \frac{\Lambda\left(s_i; k, \lambda\right)}{\sum_{n=1}^{Q} \Lambda\left(s_n; k, \lambda\right)} . \tag{3}$$

We now focus on a single bit and note that the bit is '0' for $Q/2$ of the PPM symbols and '1' for the rest. We denote the sets that contain the $Q/2$ symbols as B_ℓ^0 and B_ℓ^1, since the sets are different for the $\ell = 1, \ldots, \log_2 Q$ bits of the PPM symbol [19]. Following (3), the probability that the bit is '0' or '1' is proportional to the sum of likelihoods of the symbols in sets B_ℓ^0 and B_ℓ^1, respectively. The corresponding LLR of each bit is therefore calculated from

$$L(b_\ell) = \log\left(\frac{\sum_{i\in B_\ell^0} \Lambda\left(s_i; k, \lambda\right)}{\sum_{i\in B_\ell^1} \Lambda\left(s_i; k, \lambda\right)}\right) . \tag{4}$$

III. Results and Discussion

The performance of the system was evaluated using MC simulations. To this end, random data bits were coded using the corresponding encoder and were then converted to PPM symbols. The empty slots were mapped to randomly generated $\chi^2_{k,0}$ variables and the energy slots were mapped to randomly generated $\chi^2_{k,\lambda}$ variables. The PPM demodulator either utilized the RVs directly to produce the bitstream for the RS decoder based on maximum values, or utilized (4) to calculate the log-likelihoods for the LDPC decoder. The decoder output was compared with the original data bits and the BEP was estimated by counting the errors over multiple successive decodings.

Fig. 2 presents results for 4-PPM and $k = 2, 40$ noise modes. The uncoded system performance is obtained using [20, eq. (15)] and is included for comparison purposes. As expected, the results demonstrate that the coded BEP performance is far superior compared to the uncoded. The LDPC codes also provide a significant coding gain compared to their RS counterparts. The additional coding gain provided by the LDPCs is approximately equal to 2.5 dB for $k = 2$ noise modes and 2.0 dB for $k = 40$ noise modes when the coding rate is $1/3$. However, if the code rate is increased to $2/3$ the discrepancy between the two coding schemes reduces to 1.5 dB and 1 dB, respectively. Moreover, the LDPC data block size also affects the code performance and almost 0.5 dB is lost when blocks of small size are utilized.

16-PPM provides better results in terms of E_b/N_0, as it is shown in Fig. 3. An improvement of more than 1.5 dB is observed for the LDPCs in all noise mode and coding rate combinations when the modulation order is increased. The LDPC codes also provide better performance than the RS ones in all scenarios, however the relative gain is reduced compared to what was observed for 4-PPM. The additional LDPC gain is approximately 1.5 dB and 1.0 dB for $k = 2$ and $k = 40$ for a coding rate of $1/3$. An even smaller improvement is observed for a coding rate of $2/3$, where LDPCs provide an improvement of 0.5 dB or less, depending on the block size.

IV. Conclusion

We have presented results on the BEP performance of optically pre-amplified PPM receivers that utilize the recently proposed LDPC codes of the 5G standard, as well as RS codes. The results show that the utilization of LDPC codes drastically reduces the required E_b/N_0, especially if they are combined with a high modulation order. The LDPCs also outperform

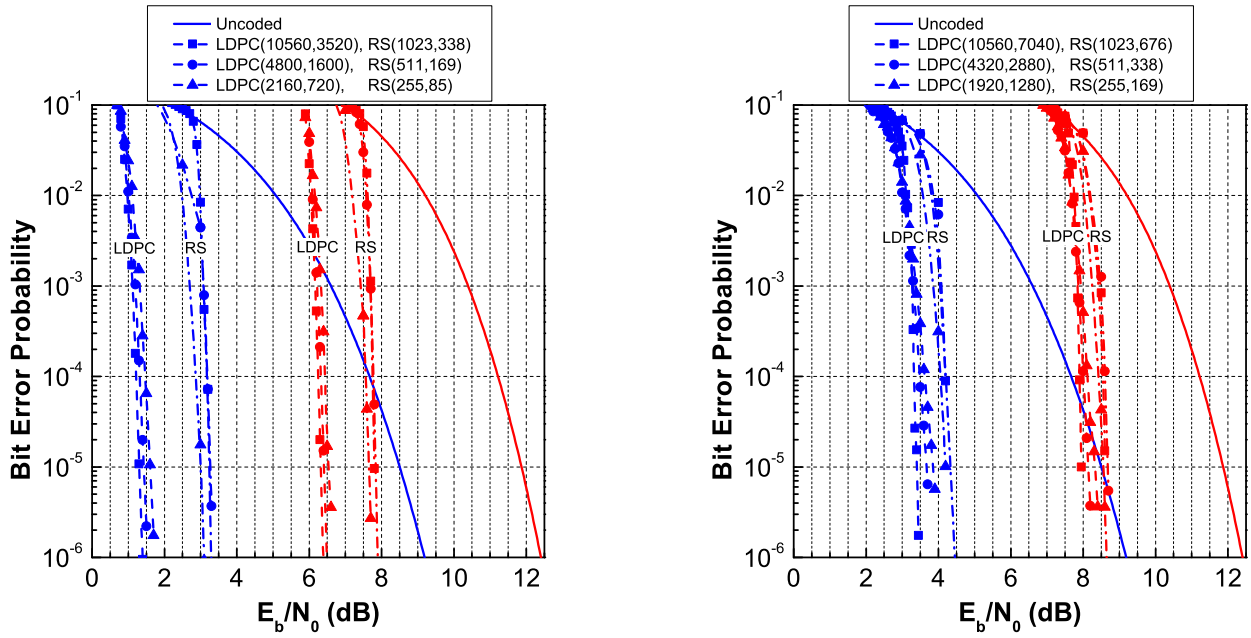

Fig. 3: BEP for the RS and LDPC coded pre-amplified 16-PPM receiver. The blue and red colors correspond to $k = 2$ and $k = 40$ noise modes, respectively.

the RS codes, but the relative improvement depends on the modulation order, noise modes and coding rate. An increase in any of those three parameters results in RS codes performing more closely to the LDPC ones.

REFERENCES

[1] D. M. Boroson, J. J. Scozzafava, D. V. Murphy, B. S. Robinson, and M. I. T. Lincoln, "The lunar laser communications demonstration (llcd)," in *2009 Third IEEE International Conference on Space Mission Challenges for Information Technology*, 2009, pp. 23–28.

[2] F. I. Khatri, B. S. Robinson, M. D. Semprucci, and D. M. Boroson, "Lunar laser communication demonstration operations architecture,," *Acta Astronautica*, vol. 111, pp. 77–83, 2015.

[3] D. O. Caplan, B. S. Robinson, R. J. Murphy, and M. L. Stevens, "Demonstration of 2.5-gslot/s optically-preamplified m-ppm with 4 photons/bit receiver sensitivity," in *Optical Fiber Communication Conference and Exposition and The National Fiber Optic Engineers Conference*. Optical Society of America, 2005, p. PDP32.

[4] M. L. Stevens and D. M. Boroson, "A simple delay-line 4-ppm demodulator with near-optimum performance," *Opt. Express*, vol. 20, no. 5, pp. 5270–5280, Feb 2012.

[5] H. Pfister, I. Sason, and R. Urbanke, "Capacity-achieving ensembles for the binary erasure channel with bounded complexity," *IEEE Transactions on Information Theory*, vol. 51, no. 7, pp. 2352–2379, 2005.

[6] T. Richardson and S. Kudekar, "Design of low-density parity check codes for 5g new radio," *IEEE Communications Magazine*, vol. 56, no. 3, pp. 28–34, 2018.

[7] S. Hu, L. Mi, T. Zhou, and W. Chen, "35.88 attenuation lengths and 3.32 bits/photon underwater optical wireless communication based on photon-counting receiver with 256-ppm," *Opt. Express*, vol. 26, no. 17, pp. 21 685–21 699, Aug 2018.

[8] I. Djordjevic, B. Vasic, and M. Neifeld, "Multilevel coding in free-space optical mimo transmission with q-ary ppm over the atmospheric turbulence channel," *IEEE Photonics Technology Letters*, vol. 18, no. 14, pp. 1491–1493, 2006.

[9] M. F. Barsoum, B. Moision, M. P. Fitz, D. Divsalar, and J. Hamkins, "Exit function aided design of iteratively decodable codes for the poisson ppm channel," *IEEE Transactions on Communications*, vol. 58, no. 12, pp. 3573–3582, 2010.

[10] H. Zhou, M. Jiang, C. Zhao, and J. Wang, "Optimization of protograph-based ldpc coded bicm-id for the poisson ppm channel," *IEEE Communications Letters*, vol. 17, no. 12, pp. 2344–2347, 2013.

[11] B. Matuz, E. Paolini, F. Zabini, and G. Liva, "Non-binary ldpc code design for the poisson ppm channel," *IEEE Transactions on Communications*, vol. 65, no. 11, pp. 4600–4611, 2017.

[12] K. Fatima, S. S. Muhammad, and E. Leitgeb, "Adaptive coded modulation for fso links," in *2012 8th International Symposium on Communication Systems, Networks and Digital Signal Processing (CSNDSP)*, 2012, pp. 1–4.

[13] D. Marcuse, "Derivation of analytical expressions for the bit-error probability in lightwave systems with optical amplifiers," *Journal of Lightwave Technology*, vol. 8, no. 12, pp. 1816–1823, 1990.

[14] P. A. Humblet and M. Azizoglu, "On the bit error rate of lightwave systems with optical amplifiers," *Journal of Lightwave Technology*, vol. 9, no. 11, pp. 1576–1582, Nov 1991.

[15] S. Sahuguede, A. Julien-Vergonjanne, and J.-P. Cances, "Soft decision ldpc decoding over chi-square based optical channels," *Journal of Lightwave Technology*, vol. 27, no. 16, pp. 3540–3545, 2009.

[16] A. Anastasopoulos, "A comparison between the sum-product and the min-sum iterative detection algorithms based on density evolution," in *GLOBECOM'01. IEEE Global Telecommunications Conference*, vol. 2, 2001, pp. 1021–1025 vol.2.

[17] N. Andreadou, F.-N. Pavlidou, S. Papaharalabos, and P. T. Mathiopoulos, "Quasi-cyclic low-density parity-check (qc-ldpc) codes for deep space and high data rate applications," in *2009 International Workshop on Satellite and Space Communications*, 2009, pp. 225–229.

[18] J. Hamkins, "Performance of binary turbo-coded 256-ary pulse-position modulation," in *TMO Progress Report 42-13*, 1999, pp. 1–15.

[19] T. Javornik, I. Jelovčan, S. Sheikh Muhammad, and G. Kandus, "Simplified soft value extraction for m-ppm-modulated signals in fso systems," *AEU - International Journal of Electronics and Communications*, vol. 63, no. 7, pp. 595–599, 2009.

[20] K. Yiannopoulos, N. C. Sagias, and A. C. Boucouvalas, "Average error probability of an optically pre-amplified pulse-position modulation multichannel receiver under malaga-m fading," *Applied Sciences*, vol. 10, no. 3, 2020.